Text and references accompanying Nevada Bureau of Mines and Geology Open-File Report 2022-09

Geologic Map of the Como Quadrangle, Lyon County, Nevada

by

Michael C. Say and Andrew V. Zuza

Nevada Bureau of Mines and Geology, University of Nevada, Reno

2022

Disclaimer: NBMG open-file reports have not been formally peer reviewed. This geologic map was funded in part by the USGS National Cooperative Geologic Mapping Program under STATEMAP award number G21AC10873, 2021.

ABSTRACT

This 1:24,000-scale geologic map of the Como 7.5-minute quadrangle covers part of the northern Pine Nut Mountains in Lyon County, Nevada. The northern Pine Nut Mountains consist of Mesozoic plutonic and sedimentary rocks unconformably overlain by west-tilted Oligocene tuff and a thick-package of Miocene volcanic and sedimentary strata. The range was tilted westward by Miocene east-dipping normal and left-oblique faulting along the middle and eastern flanks of the Pine Nut Mountains.

The map area consists mostly of parallel and conformable west-tilted Miocene volcanic and sedimentary rocks that are ~2 km thick. The volcanic sequence consists of mostly dacite to andesite, with some basaltic andesite. Some dacite-andesite dikes intrude the volcanic rocks. New $^{40}Ar/^{39}Ar$ dates bracket main volcanic sequence to 14.2–6.8 Ma, with most dates between 8.2 and 6.8 Ma. Miocene strata were deposited on sparse Oligocene ash-flow tuff and the Jurassic Gardnerville Formation. The Miocene sequence was tilted 30°–36° west by several north-striking east-dipping normal faults that must have initiated after ca. 6.8 Ma based on the parallel nature of the volcanic section. Restoration of the faulted strata suggests >14% extensional strain.

The Como Mining District is located in the northern Pine Nut Mountains and hosts gold and silver mineralization. Active exploration projects are currently underway throughout the range including the Hercules project. Mineralization is thought to be a low-sulfidation volcanic-hosted epithermal gold and silver deposit. Abundant northeast-striking quartz veins are exposed throughout the Como, Hercules, and eastern flank areas. Large halos of hydrothermally altered volcanic rock envelope quartz veins. Alteration is not observed in the hanging wall of the main eastern fault block.

DESCRIPTION OF MAP UNITS

Quaternary Deposits

Qc Colluvium (Holocene to late Pleistocene) Angular to slightly rounded, poorly sorted boulders to pebbles in a variably sandy matrix. Present at the base of steep bedrock slopes.

Qa Active alluvium (Holocene) Coarse, clast supported and poorly sorted light-colored (absent varnish) cobble clasts to sand grains. Curvilinear features displaying relatively low relief to all adjacent forming deep canyons in bedrock in some regions of the map area. Occasional linear ridges composed of cobbles and boulders (debris-flow levees). Qa dissects all units and incision amount depends on incised unit age. Distinguished in aerial imagery by light tone contained in linear to wavy features incised in units of all ages.

Qsa Spring deposits (Holocene) White-colored silt, sand, carbonate, and gypsum adjacent to natural springs and along fault traces in the western portion of the map area. Display very high albedo in satellite imagery relative to adjacent units.

Qpl Playa deposits (Holocene) Fine silt and clay deposits. Circular to round deposits exposed in the topographically lowest regions of basins throughout the map area. Deposits display high albedo in satellite imagery relative to adjacent deposits. Qpl deposits are found throughout the central-eastern portion of the map area in ridge bounded basins and are seasonal lakes.

Qfy Youngest alluvial-fan deposits (Holocene) Deposits of silt, sand, and pebble- to cobble-sized gravels. Conical shaped lobes composed of poorly sorted subangular pebbles to sparse cobbles, displaying absent varnish on clasts. Display fresh bar-and-swale surface morphology with linear ridges. Lower elevation than older, adjacent fan units. Distinguished in aerial imagery by lighter tone than similar units of Qfi and Qfo.

Qao Old inactive alluvium, colluvium, talus, and basin fill (Holocene) Colluvium and talus deposits occur as conical shaped lobes located at the base of steep slopes of bedrock throughout the map area. Inactive alluvium deposits occur adjacent to active channels within small canyons. Basin-fill deposits are exposed in low elevation areas in the central-eastern portion of the map area, contained in ridge-bounded basins and display broad, very flat surfaces of silt and sand.

Qls Landslide deposits (late Pleistocene to Holocene) Undulating and hummocky broad surfaces of poorly sorted colluvium and bedrock float up to several meters in diameter. In the northwest portion of the map area, Qls deposits cover bedrock and contain portions of Tad float that were transported from higher elevations into lower elevations during mass-wasting events creating a hummocky landscape of irregular exposures of bedrock. Other Qls deposits throughout the map area are exposed adjacent to steep slopes of bedrock that display landslide scars.

Qfi Intermediate alluvial-fan deposits (late Pleistocene to Holocene) Deposits of silt, sand, and pebble- to cobble-sized gravels. Broad, mostly flat surfaces with small incised channels by active alluvium. Surfaces are matrix supported and composed of poorly sorted subangular to subrounded gravels and cobbles displaying moderate to poor varnish development. Qfi deposits are exposed throughout the map area and are lower in elevation than Qfo deposits and higher in elevation that Qa and Qfy deposits.

Qp Pediment deposits (late Pleistocene?) Deposits of silt, sand, and pebble- to cobble-sized gravels. Broad flat surfaces that occur mostly on the eastern flank of the main range near the center of the map area. These surfaces are composed of moderate to poorly sorted subangular gravels and cobbles with occasional rounded boulders displaying well-developed varnish. Surfaces are deeply incised (up to 100 m) by active channels. Qp exposures directly overlie bedrock and in some areas are a thin veneer capping bedrock exposed along incised channels

Qla Lacustrine and eolian modified alluvial fans (late Pleistocene?) Deposits of silt, sand, and pebble- to cobble-sized gravels. Broad surfaces that are deeply incised by inactive and active channels. Rounded crests and sparse pavement development is present in some areas. Surfaces are composed of subrounded cobbles and gravels that are possibly lacustrine beach deposits that have been modified by eolian processes. Potential curvilinear shorelines are visible on satellite imagery as dark bands with lighter high albedo bands between deposits that follow contours. A clear lacustrine shoreline deposit visible on satellite imagery is indicated in the northeast portion of the map area.

Qfo Older alluvial-fan deposits (middle to late Pleistocene?) Silt, sand, and pebble to cobble-sized gravels. Broad, flat surfaces with incised channels; channel ridges display very rounded crests, matrix supported consisting of subangular to angular gravel to boulders displaying well-developed varnish and pavement development. Qfo deposits are incised by and are higher in elevation than younger alluvial fans. Deposits are found throughout the map area adjacent to flanks of the main range near canyon mouths and smaller ridges in the east.

Tertiary Igneous and Sedimentary Rocks

The dominant bedrock lithology consists of Miocene volcanic rocks that are intermediate to felsic (~55%–65% SiO_2) (fig. 1), calc-alkaline, and predominately metaluminous (Say and Zuza, 2021). All samples are consistent with being generated within an arc-subduction zone (e.g., Pearce, 2008; Pearce and Peate, 1995) based on their trace element data (i.e., Nb depletion and Sr, K, and Ba enrichment) and are broadly similar to other studied volcanic rocks associated with the ancestral Cascade arc around the greater Reno, Nevada, region (Cousens et al., 2008; du Bray and John, 2011; Timmermans et al., 2020). It is interpreted that volcanism in the Pine Nut Mountains was related to the ancestral Cascade arc and preceded Basin and Range bimodal volcanism in the area. The naming and dates for most units are based on Say and Zuza (2021, 2020), although some units have been updated for this map publication.

Tcc Cobble conglomerate (late Miocene) Andesite cobble conglomerate deposited on the upper Tba unit and exposed in the north-central portion of the map area. Sparse reworked biotite tuff is exposed along the basal section of the unit. Complete unit thickness is unknown.

Tdi Intrusive porphyritic dacite (late Miocene) Porphyritic dacite shallow intrusive domes, volcanic vents and vent breccia, and dikes are composed of coarse euhedral hornblende (up to 1 cm), plagioclase, and light-gray groundmass. Tdi intrusive domes in the northwest section of the map area are redder in color and are silicified in some areas. Two $^{40}Ar/^{39}Ar$ hornblende dates are 6.59 ± 0.06 Ma from a Tdi dike and 6.89 ± 0.05 Ma from an intrusive dome (Say and Zuza, 2021).

Tai Intrusive porphyritic andesite (late Miocene) Porphyritic andesite shallow intrusive domes and volcanic vents display hornblende, plagioclase, sparse clinopyroxene, and a dark gray groundmass. Tai exposures typically display alteration, and in some cases, are highly foliated with foliation attitudes drastically different than the foliation of rock Tai intruded.

Tba Andesite and basaltic andesite flows (late Miocene) Dark gray to gray porphyritic andesite and aphanitic basaltic andesite (~56–59% SiO_2) flows and flow breccias. This unit directly overlaps, or is interpreted to overlap, most of the older Miocene rocks in the study area, and unconformably overlies units with substantial structural relief, from Tss to Tcs. Tba is also less tilted than most of the other units, evidenced by its lower, more moderate dips. These observation suggest that Tba may have been deposited during or after significant extension and block rotation that tilted the units in the map area. Two groundmass $^{40}Ar/^{39}Ar$ dates were 6.99 ± 0.10 Ma and 6.77 ± 0.02 Ma (Say and Zuza, 2021). The structural relationships and less deformed nature of Tba suggests that ca. 6.77 Ma may be a more meaningful date for the unit, which is younger than the ca. 6.83 Ma age of the more tilted Tad unit (Say and Zuza, 2021). This constrains much of the normal faulting and exhumation of the Pine Nut Mountains footwall block to ca. 6.8 Ma, after the deposition of Tad and before the deposition of Tba.

Tad Porphyritic dacite and andesite flows, related interbedded volcaniclastic, undivided (late Miocene) Thick flows of porphyritic dacite and thin flows of aphanitic andesite. Andesite flows are sparse and are found in the lower section of the unit. The flows are dark gray in color and foliated. Porphyritic dacite flows comprise the majority of the unit with the thickest flows (over 30 m thick) near the upper portion of the unit in the western portion of the map area. Tad is poorly exposed in the east of the map area and outcrops are typically piles of Tad float on ridges. The dacite flows are gray to light gray in color and are composed of coarse hornblende, coarse plagioclase, quartz, rare biotite, and groundmass. Subrounded xenoliths of rounded andesite and dacite are abundant throughout the unit. Interbedded volcanic debris flows and cobble conglomerates (up to 5 m thick) composed of dacite and andesite clasts are present throughout Tad in the eastern and western portions of the map area. A biotite $^{40}Ar/^{39}Ar$ age was 6.83 ± 0.014 Ma and a hornblende $^{40}Ar/^{39}Ar$ age was 7.15± 0.10 Ma (Say and Zuza, 2021). Tad is parallel to the underlying late Miocene volcanic and sedimentary rocks, and thus it is interpreted that significant normal faulting and regional extension did not initiate until after the deposition of this unit at ca. 6.83 Ma (Say and Zuza, 2021). The upper contact is not exposed in the study area, but this unit may be >1.5 km thick.

Tbatu Upper block-and-ash tuff (late Miocene) Block-and-ash tuff composed of boulder to pebble subangular to subrounded clasts in a dull green, blue, purplish tuffaceous matrix. Clast types range from tuff fragments to porphyritic andesite. Tbatu host abundant surficial alteration and mineralization in the Hercules area. Tbatu and Tbatl are very similar in composition and appearance; however, a thin <10 m porphyritic andesite flow at the base of Tbatu divides the two tuffs, and in other areas, unit Tbhf divides the units. Tbatu also contains less sedimentary reworking textures than what has been observed within Tbatl. Up to 250 m thick.

Tbhf Biotite hornblende volcanic flows (late Miocene) Porphyritic volcanic flows and crystal tuffs containing phenocrysts of hornblende (up to 2 cm), biotite (5 mm), and feldspar (5 mm) in a light gray to bleached white (sericitized?) groundmass. Hornblendes are clay altered and chloritized, feldspars are clay altered and biotite appears unaltered. Weathered outcrops are typically white to light gray and display a rounded exfoliative weathering pattern. Flow banding and columnar jointing are observed in tilted exposures. Thin Tbhf flows rarely outcrop within Tbatl near the contact of the two units suggesting interfingering during deposition. Unit pinches out to the north and south and likely deposited in a paleo-low. This unit is typically <100 m thick.

Tbatl Lower block-and-ash tuff (late Miocene) Monomict and polymictic block and ash tuffs, pyroclastic debris flows, and tuffaceous sandstone, siltstone, and mudstones. Tbatl is exposed in the central to northern half of the map area and is a primary unit to host alteration and mineralization likely due to high permeability of the unit. Tbatl appears to pinch out to the south along strike near the historic Como townsite. Unit is commonly propylitically altered outcropping in a dull blue to dull purple in color. Block-and-ash tuffs contain boulder- to-pebble sized subrounded to subangular purplish porphyritic andesite and bleached (?) light-gray hornblende-bearing andesite clasts in tuffaceous matrix that contain phenocrysts of hornblende and plagioclase. Biotite is rarely present in the matrix and in some clasts. Beds of reworked tuffs that display sedimentary features have been observed throughout the unit. Tuffaceous, coarse-grained sandstones and siltstone occur near the base of the unit specifically in the NE section of the map where the unit is exposed. The thickness of the overall unit is up to 100 m in some areas but likely varies throughout the area.

Tac Como andesite (late Miocene) The Como andesite unit (58%–64% SiO_2) is comprised of andesite flows, interbedded reworked tuff, and pyroclastic flow deposits (unit Tact). The base of the unit is not exposed and varies in thickness along strike, but an estimate of the minimum thickness is 1 km. Tac outcrops in flows and intercalated reworked tuff to tuffaceous breccias that have undergone hydrothermal alteration. In the upper Tac unit, the interbedded, reworked tuff are propylitically altered displaying montmorillonite ± quartz ± calcite ± chlorite ± pyrite ± epidote. Andesite flows near the base of the unit exhibit equigranular phenocrysts and thin laths of hornblende while upper portions of the unit contain porphyritic flows that have coarser, more variable phenocrysts with larger hornblende crystals up to 1 cm. Some hornblende grains are oxidized to magnetite or contain magnetite rims. Some aphanitic basaltic andesite flows are present in the unit and contain clinopyroxene (augite?) and orthopyroxene phenocrysts. Hornblende are sparse or completely absent from the basaltic andesite flows. $^{40}Ar/^{39}Ar$ hornblende date from the lower portion of Tac yielded an age of 7.30 ± 0.09 Ma (Say and Zuza, 2021). The unit is up to ~1 km thick.

Tact Interbedded reworked tuff and volcanic breccia (late Miocene) Discontinuous interbeds of reworked lithic tuff, block-and-ash tuff, and pyroclastic debris flows in unit Tac. Massive, poorly sorted, rounded to subangular clasts of porphyritic Como andesite (Tac) ranging in size from 1 cm to 1 m are supported by a tuffaceous matrix with feldspar crystal fragments. The tuffaceous matrix exhibits a pale green to pale purplish blue in color. Propylitic alteration has obscured much of the original layering structure, if originally present. The alteration mineral assemblage in this member is largely chlorite ± calcite ± pyrite ± montmorillonite (Vikre and McKee, 1994). Exposures are typically small and discontinuous lenses that weather and erode easily as opposed to more competent andesite flows of Tac. Sparse, reworked sedimentary features that display bedding are found throughout this unit. Thickness varies from 5 m to ~100 m.

Tvc Andesitic conglomerate, volcanic breccia, and volcaniclastic sandstone (late Miocene) subangular to subrounded boulder- to cobble-sized andesite clasts in a sandy-ash matrix. The lower portion of the unit contains channels of massive, tan-colored sandstone and pyroclastic-flow deposits exhibiting 5 cm angular clasts of dull green tuff. A 5-m-thick flow of aphanitic black to dark-gray andesite is poorly exposed in the lower portion of the unit.

Tvcu Volcaniclastic deposit, undivided (middle to late Miocene?) Pale bluish-green to pale purple colored volcaniclastic deposit composed of matrix-supported angular to subrounded clasts of andesite and tuff in some areas. Matrix is composed of sand and silt. Alteration has destroyed much of the original bedding, but bedding is present in some areas of the map. Includes a poorly exposed, but apparently interbedded dark gray to black colored aphanitic andesite composed with fine plagioclase visible in groundmass. Alteration and deformation make correlation of this unit with others challenging.

Tss Mudstone and diatomaceous siltstone (late Miocene) Gray thinly laminated diatomite, mudstone, and siltstone. Outer surfaces of the mudstone weather to tan-brown in color. The unit is occasionally opalized and silicified in some areas. Approximately 20–30 m thick.

Tcb Volcaniclastic and lahar channels (middle to late Miocene) Black lahar and conglomerate discontinuous channels. Composed of clast-supported angular black aphanitic basaltic andesite (up to 10 cm in diameter) in a black matrix composed of mud and silt. Discontinuous channels roughly 10 m thick.

Thd Porphyritic hornblende dacite (middle Miocene) Dark gray to gray porphyritic dacite (64%–66% SiO_2) composed of hornblende, plagioclase (up to 4 mm), and sparse quartz and xenoliths (up to 5 mm). Distinguished by 0.5 cm highly chloritized hornblende found throughout the unit. Thd are likely temporally related to unit Tbd. The unit is approximately 250–300 m thick.

Tcs Conglomerate and silicified sediments (middle to late Miocene?) Light tan to brown-colored matrix-supported cobble conglomerate. Cobbles are composed of rounded porphyritic andesite clasts (up to 30 cm) in a lighter-colored sand and tuffaceous matrix. Lower section contains silicified tuffaceous sediments, chert pebble conglomerate, and pale bluish-purple volcaniclastic sediments. Thickness is variable but is up to ~ 300(?) m thick.

Tdf Dacitic volcanic flows (middle to late Miocene) Porphyritic dacite flows composed of hornblende, feldspar, biotite, and quartz in glassy gray groundmass. These flows occur above and rarely intercalated with Tdbat, which is composed of Tdf clasts. Flow banding is visible throughout the unit, specifically on weathered surfaces. A hornblende $^{40}Ar/^{39}Ar$ date was 8.20 ± 0.05 Ma (Say and Zuza, 2021).

Tdbat Intercalated block-and-ash tuff and pyroclastic flow (middle to late Miocene) Bedded, monomict block-and-ash tuff, matrix supported with subangular clasts of porphyritic hornblende, feldspar, biotite, and quartz (unit Tdf) suspended in a tuffaceous, glassy gray matrix.

Tbd Porphyritic biotite dacite (middle Miocene) Gray porphyritic dacite (~64% SiO_2) composed of plagioclase, coarse euhedral biotite (up to 5 mm), sparse quartz and hornblende. Flow foliation in outcrops are poorly exposed and are highly weathered. $^{40}Ar/^{39}Ar$ biotite dating yielded an age of 14.20 ± 0.012 Ma (Say and Zuza, 2021).

Tbt Biotite ash-flow tuff (late Oligocene?) Crystal rich, moderately to strongly welded ash-flow tuff (~68% SiO_2) containing sanidine, plagioclase, hornblende, quartz, and abundant euhedral biotite. Contains white pumice lapilli, sparse angular andesitic lithics up to 1 cm, abundant vesicles, and is highly foliated. Pale pink to white in color. Approximate thickness is 50 m. Based on its location and phenocryst assemblage, Tbt is most similar to either the ca. 27 Ma Lenihan Canyon or Mickey Pass Tuffs (e.g., Stewart, 1999; Henry and John, 2013). The relative abundance of biotite and the SiO_2 content are more similar to those of the 26.94 Ma Lenihan Canyon Tuff (Henry and John, 2013).

Jurassic Sedimentary Rocks

JŦg Gardnerville Formation (Triassic? to Jurassic) Metasedimentary rocks are comprised of thinly bedded gray to tan colored shale, massive, gray limestone that is intensely veined, arkose sandstone, and volcanic breccia. Outcrops along incised channels while the majority outcrops as shale chip float. The Gardnerville Formation has been biostratigraphically dated to the Jurassic age, Toarcian (Noble, 1962; Stewart, 1999). Total thickness of the formation is not exposed in the study and is likely more than several kilometers thick (Noble, 1962). Zircon analyses suggest that the maximum age of the arkosic sandstone and volcanic breccia member of the Gardnerville Formation is 177 ± 1 Ma (Say and Zuza, 2020).

ACKNOWLEDGMENTS

Research supported by the U.S. Geological Survey, National Cooperative Geologic Mapping Program, under USGS award number G21AC10873. The views and conclusions contained in this document are those of the authors and should not be interpreted as necessarily representing the official policies, either expressed or implied, of the U.S. Government. This map was made during the masters research by the first author, with support and guidance from faculty, students, and staff at the University of Nevada, Reno. Matt Heizler is thanked for assistance with argon analyses at New Mexico Tech. Additional mapping was conducted by a mineral exploration company when exploring the area with help from Rocky Allen, Ron Kieckbusch, Warwick Board, Mike Allen, Joseph Mulvaney-Norris, Sean Ingersoll, and Kyle Larson. We greatly appreciated reviews by an anonymous reviewer and Joseph Colgan on a manuscript based on this mapping that improved our interpretations of the geology.

REFERENCES

Cousens, B., Prytulak, J., Henry, C., Alcazar, A., and Brownrigg, T., 2008, Geology, geochronology, and geochemistry of the Miocene–Pliocene ancestral Cascades arc, northern Sierra Nevada, California and Nevada—the roles of the upper mantle, subducting slab, and the Sierra Nevada lithosphere: Geosphere, v. 4, no. 5, p. 829–853.

du Bray, E.A., and John, D.A., 2011, Petrologic, tectonic, and metallogenic evolution of the ancestral Cascades magmatic arc, Washington, Oregon, and northern California: Geosphere, v. 7, no. 5, p. 1102–1133.

Henry, C.D., and John, D.A., 2013, Magmatism, ash-flow tuffs, and calderas of the ignimbrite flareup in the western Nevada volcanic field, Great Basin, USA: Geosphere, v. 9, no. 4, p. 951–1008.

Irvine, T.N., and Baragar, W.R.A., 1971, A guide to the chemical classification of the common volcanic rocks: Canadian Journal of Earth Sciences, v. 8, no. 5, p. 523–548.

Le Bas, M.J., Le Maitre, R.W., Streckeisen, A., and Zanettin, B., 1986, A chemical classification of volcanic rocks based on the total alkali-silica diagram: Journal of petrology, v. 27, no. 3, p. 745–750.

Noble, D.C., 1962, Mesozoic geology of the Southern Pine Nut Range, Douglas County, Nevada: Stanford, California, Stanford University (PhD dissertation), p. 200

Pearce, J.A., 2008, Geochemical fingerprinting of oceanic basalts with applications to ophiolite classification and the search for Archean oceanic crust: Lithos, v. 100, no. 1–4, p. 14–48.

Pearce, J.A., and Peate, D.W., 1995, Tectonic implications of the composition of volcanic arc magmas: Annual Review of Earth and Planetary Sciences, v. 23, no. 1, p. 251–285.

Say, M.C., and Zuza, A.V., 2020, Late Miocene transition between Basin and Range extension and Walker Lane tectonics, northern Pine Nut Mountains, Nevada—new insights from Geologic Mapping: 2020 Vision for Discovery Symposium, p. 1351–1374.

Say, M.C., and Zuza, A.V., 2021, Heterogenous late Miocene extension in the northern Walker Lane (California-Nevada, USA) demonstrates vertically decoupled crustal extension: Geosphere, v. 17, no. 6, p. 1762–1785.

Stewart, J.H., 1999, Geologic map of the Carson City 30 X 60 minute quadrangle, Nevada: Nevada Bureau of Mines and Geology, scale 1;100,000.

Sun, S.S., and McDonough, W.F., 1989, Chemical and isotopic systematics of oceanic basalts—implications for mantle composition and processes: Geological Society, London, Special Publications, v. 42, no. 1, p. 313–345.

Timmermans, A.C., Cousens, B.L., and Henry, C.D., 2020, Geochemical study of Cenozoic mafic volcanism in the west-central Great Basin, western Nevada, and the ancestral Cascades arc, California: Geosphere, v. 16, no. 5, p. 1179–1207.

Vikre, P.G., and McKee, E.H., 1994, Geology, alteration, and geochronology of the Como district, Lyon County, Nevada: Economic Geology, v. 89, no. 3, p. 639–646.

Suggested citation:

Say, M.C., and Zuza, A.V., 2022, Geologic map of the Como quadrangle, Lyon County, Nevada: Nevada Bureau of Mines and Geology Open-File Report 2022-09, scale 1:24,000, 7 p.

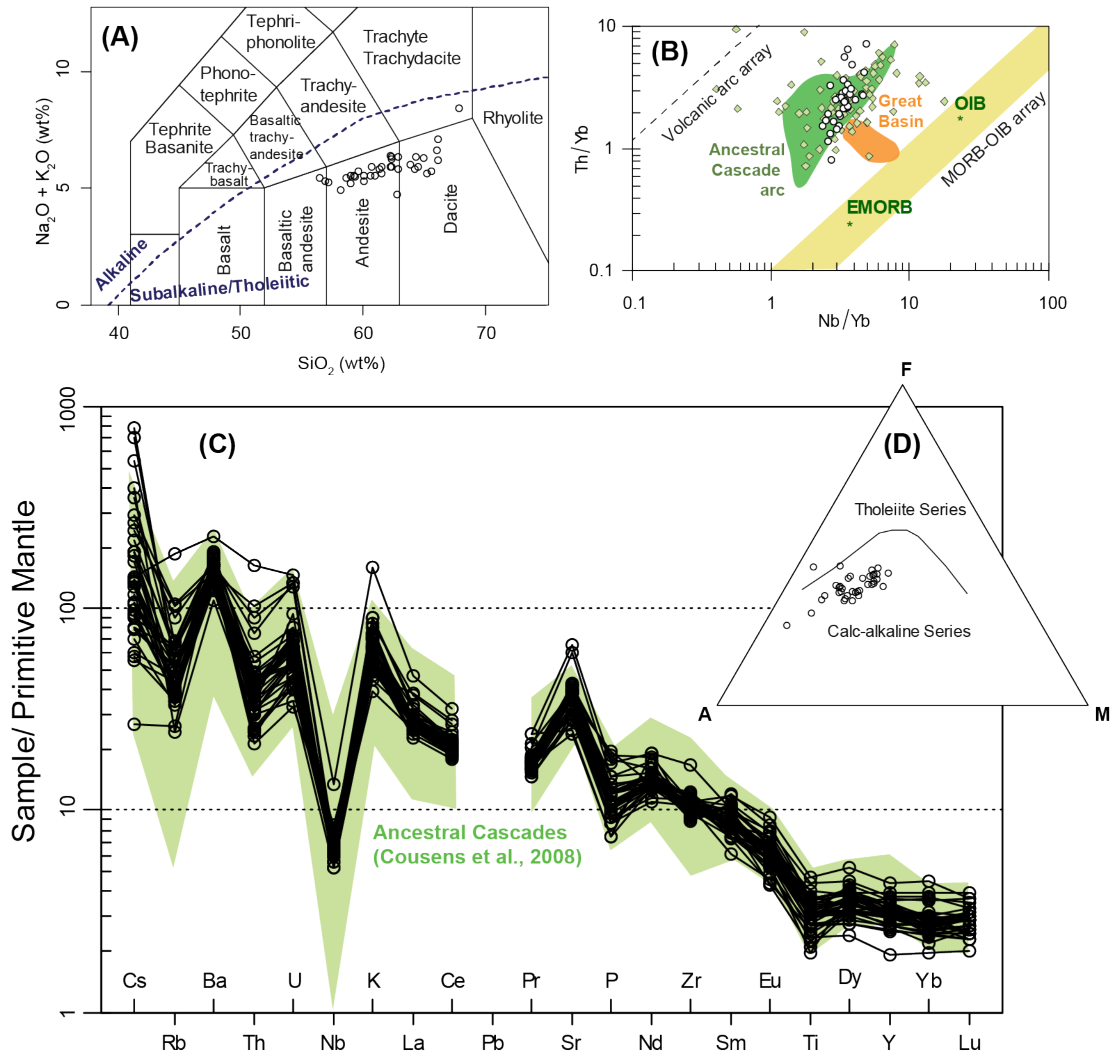

Figure 1. Geochemistry from the northern Pine Nut Mountains from Say and Zuza (2020, 2021). (A) Total alkalis versus silica (TAS) diagram of Le Bas et al. (1986). (B) Geochemical discrimination diagram of Pearce (2008), plotted as black-outlined white circles with ancestral Cascade arc data from Cousens et al. (2008) (green symbols) and Timmermans et al. (2020) (green field). Also plotted is Great Basin volcanic rocks (orange field) from Timmermans et al. (2020). MORB—mid-ocean ridge basalt; EMORB—enriched MORB; OIB–ocean island basalt. (C) Primitive mantle normalized (Sun and McDonough, 1989) trace element spider diagram of the sampled northern Pine Nut Mountains magmatic suite. Ancestral Cascade arc data from volcanic rocks sampled from the Lake Tahoe-Reno, NV region plotted as green field from Cousens et al. (2008). (D) AFM (Na_2O+K_2O–FeO–MgO ternary) plot with tholeiite versus calc-alkaline divisions of Irvine and Baragar (1971).

Table 1. $^{40}Ar/^{39}Ar$ ages for samples from the northern Pine Nut Mountains (Say and Zuza, 2021)

Sample	Map unit	Latitude	Longitude	Analyzed phase	Preferred Age (Ma)	Uncertainty (Ma)
MS-261018-2*	Tad	39.16056	119.51802	H	7.15	0.1
MS-270918-1	Tac	39.18904	119.45032	H	7.30	0.09
MS-220918-1	Tba	39.24242	119.39303	G	6.77	0.02
MS-070719-4	Tba	39.22924	119.43229	G	6.99	0.1
MS-240819-4	Tdi	39.23125	119.44416	H	6.89	0.05
MS-060419-4	Tdi	39.19499	119.44747	H	6.59	0.06
MS-240819-3	Tbf	39.23464	119.43358	H	8.20	0.05
MS-230619-1	Tad	39.19783	119.48931	H	-	-
MS-030819-1B*	Tad	39.20418	119.51380	H	-	-
MS-240819-6b*	Tbd	39.24570	119.50240	B	14.20	0.02
MS-070819-4	Tad	39.18691	119.42935	B	6.83	0.01

Note: Analyzed phases: H—hornblende; G—groundmass; B—biotite. Dash indicates sample displayed disturbed spectra and thus no single age is reported.
*Resides outside of map extent